# Front propagation in one-dimensional autocatalytic reactions: The breakdown of the classical picture at small particle concentrations

J. Mai, I. M. Sokolov, and A. Blumen
*Theoretische Polymerphysik, Universität Freiburg, Hermann-Herder Strasse 3, D-79104 Freiburg im Breisgau, Germany*
(Received 26 January 2000)

The autocatalytic scheme $A+B\xrightarrow{p}2A$ in a discrete particle system is studied in one dimension via Monte Carlo simulations. We find considerable differences in the results for the front velocities and front forms compared to the classical, continuous picture, which is only valid in the limit of very small reaction probabilities $p$. Interestingly, we also obtain front propagation velocities fairly below the classical minimal velocity.

PACS number(s): 05.40.−a, 82.20.Mj, 82.65.−i

## I. INTRODUCTION

Reaction kinetics in low dimensions were extensively investigated in the past two decades, since they differ significantly from the situation in high-dimensional spaces, and often violate strongly the classical (mean-field) kinetical schemes based on the mass-action law [1,2]; this happens in particular for $d=1$ and 2, where the reaction terms show a strong dependence on high-order particle correlation functions [3,4].

In this paper, we investigate the front propagation in the autocatalytic scheme $A+B\xrightarrow{p}2A$, where $p$ is the reaction probability of an $A$ with a $B$ particle. The system is studied in one dimension (1D) by Monte Carlo simulations and by analytical methods taking into account the particulate nature of the system.

The classical picture dating back to Fisher and to Kolmogorov, Piskunov, and Petrovsky describes the propagation within the continuous reaction-diffusion equation scheme [5,6]. This scheme predicts the existence of a minimal front velocity $v_{\min}$, which under a wide range of conditions should be the only velocity sustained by the system.

Discreteness effects, however, can strongly alter the reaction's behavior, here in particular the front's velocity [7–17]. The particulate nature means that the local concentrations are discrete, a fact that influences the concentration fluctuations. Furthermore, discreteness means that particles of the ''wrong'' kind can be found only at a finite distance from the position of the front, leading to a cutoff of concentration [18]. Both these effects typically give rise to velocities larger than $v_{\min}$ [5,6]. Numerical simulations in one-dimensional systems with high particle concentration under a parallel update rule [19] confirm that typically attained front velocities are larger than $v_{\min}$ and that they tend to $v_{\min}$ as the local reaction rate tends to zero.

In what follows, we investigate the situation under low particle concentrations on a one-dimensional lattice. Per unit time, each particle performs on the average one step to one of the neighboring sites. If two particles of a different kind occupy the same lattice site, they react with the probability $p$ per unit time according to $A+B\to 2A$. There is no excluded volume. At the beginning, the lattice is filled randomly with $B$ particles with concentration $C$. A single $A$ particle is located at the left border of the lattice. We show that under low concentrations and for rather small but nonzero probabilities $p$, the attained front velocity can be considerably smaller than $v_{\min}$. The value of $v_{\min}$ is obtained only in the limiting case $p\to 0$.

We also discuss the shape of the front and show that it depends strongly on the definition of the comoving frame used, and that it is in any case different from the classical prediction.

The paper is structured as follows. In Sec. II we recall Fisher's equation and its solutions and in Sec. III we discuss the velocity of a reaction front for finite reaction probabilities $p$. In Sec. IV we compare the classical results of the front's velocity with our Monte Carlo simulations. Section V deals with the shape of the front.

## II. THE FISHER EQUATION

The reaction process under consideration in the framework of a Master equation for the numbers $A(i),B(i)$ of particles at site $i$ reads

$$\frac{\partial A(i,t)}{\partial t}=\frac{1}{2}A(i-1,t)+\frac{1}{2}A(i+1,t)-A(i,t)+pAB(i,t) \tag{1}$$

and

$$\frac{\partial B(i,t)}{\partial t}=\frac{1}{2}B(i-1,t)+\frac{1}{2}B(i+1,t)-B(i,t)-pAB(i,t), \tag{2}$$

where $AB(i,t)$ is the number of $AB$ pairs on site $i$. Under a decoupling (mean-field) assumption, $AB(i,t)=A(i,t)B(i,t)$. In the continuum limit $A(i,t)\to A(x,t)$ and $B(i,t)\to B(x,t)$, one can rewrite Eqs. (1) and (2) as a single equation for the continuous concentration $A(x,t)$:

$$\frac{\partial A}{\partial t}=D\frac{\partial^2 A}{\partial x^2}+kA(C-A), \tag{3}$$

by noticing that for initial conditions corresponding to a homogeneous population of the lattice by $B$ particles, $B(i)=C$, Eqs. (1) and (2) imply $A(i,t)+B(i,t)=C=\text{const}$.

 

Equation (3) is the standard Fisher equation for the quadratic autocatalysis problem in one dimension. Here $C$ is the initial concentration of $B$, and the diffusion coefficient and the reaction rate are $D=1/2$ and $k=p$, respectively. The parameters of the Fisher equation defining the characteristic natural scales for length and time are $W=\sqrt{D/kc}=(2pc)^{-1/2}$ (front's width) and $T=(kc)^{-1}=(pc)^{-1}$. By an appropriate change of variables, Eq. (3) can be put into the dimensionless form

$$\frac{\partial y}{\partial \theta}=\frac{\partial^2 y}{\partial \xi^2}+y(1-y), \tag{4}$$

where $y=N/C$, $\xi=x/W$, and $\theta=t/T$.

Looking for a stable traveling front solution, one changes into a comoving frame, which leads to the time-independent equation

$$\frac{\partial^2 y}{\partial \xi^2}+v\frac{\partial y}{\partial \xi}+y(1-y)=0, \tag{5}$$

where the velocity $v$ has as a natural unit $V=\sqrt{Dkc}=\sqrt{pc/2}$.

Now, considering the stable propagation, we can concentrate on the behavior of the stationary solution $y(\xi)$. The explicit form of the solution of Eq. (5) is known only for a special value of $v$ and is not of physical relevance. On the other hand, the asymptotic forms of the solutions near the midpoint of the front (inflection point) and at the front's far edge are easy to obtain. In the middle of the front, near its inflection point, the term with the second spatial derivative is small and can be neglected, thus leading to a first-order equation

$$v\frac{\partial y}{\partial \xi}+ky(1-y)=0 \tag{6}$$

whose solution provides a reasonably good approximation for the central part of the front [5]. Thus, at intermediate $\xi$,

$$y(\xi)=\frac{1}{1+\exp(\xi/v)}. \tag{7}$$

This form is physically reasonable for any value of velocity $v$. On the other hand, far from the front's midpoint (at $\xi \gg v$) one can neglect the $y^2$ term and solve the linearized equation

$$\frac{\partial^2 y}{\partial \xi^2}+v\frac{\partial y}{\partial \xi}+y=0. \tag{8}$$

The solution of this equation is an exponential function:

$$y(\xi)=a\exp(-\lambda(v)\xi), \tag{9}$$

where $\lambda(v)$ is a solution of a characteristic equation

$$\lambda^2+v\lambda+1=0 \tag{10}$$

and reads

$$\lambda_{1,2}=\frac{v}{2}\pm\sqrt{\frac{v^2}{4}-1}. \tag{11}$$

The concentration $y(x)$ then only stays real if $v$ is equal to or is larger than $v_{\min}=2$ (where $v_{\min}=2\sqrt{Dkc}=\sqrt{2pc}$ in the initial units); this is a lower bound on $v$. The marginal stability principle then states that $v=v_{\min}$. The corresponding $\lambda$ is then $\sqrt{2/pc}$. Equation (9) is the concentration profile in the far tail region, and the overall front form can be obtained as an interpolation between Eq. (7) and Eq. (9).

## III. THE VELOCITY OF THE FRONT

In our simulations we use lattices of size $L=3000$ and follow each realization of the process until the front reaches the middle of the lattice. We use reflective boundary conditions at both ends of the lattice. The values of $p$ vary between 0.0005 and 0.3. Depending on $p$, we perform between 500 and 10 000 independent runs.

The velocity of the front can be defined using three procedures implying different averaging assumptions.

(i) One can fix the time $t$ and calculate the average concentration profile of the front. The front's position $x(t)$ is then defined as the point where $A(x(t))=C/2$ and the velocity is $v=x(t)/t$. This method does not allow us to define the front velocity in each realization separately. This is rendered possible by the following two definitions.

(ii) One determines the position of the rightmost $A$ particle (RAP) in each realization and calculates $v$ from $x(t)=x_{RAP}(t)$, again as $v_{RAP}(t)=x_{RAP}(t)/t$.

(iii) Another possibility is given through the total number $N_A(t)$ of $A$ particles at time $t$: We then set $x(t)=N_A(t)/C$.

Different procedures imply different types of averaging. The velocities obtained by (i) are already averaged over all realizations. In method (ii), $v_{\mathrm{RAP}}$ depends on the specific realization; the result obtained by (iii) is in some sense preaveraged. We find that the mean velocities obtained through these three procedures coincide with each other within 1%, but their fluctuation properties differ; see the next section.

We have performed a series of simulations using all three methods. In each case the position of the front, after a short transient, starts to grow linearly in time, and the propagation of the front is stable. The parameters of our simulations are always chosen to allow for simulation times much longer than the transient.

We start by presenting results of our numerical simulations in Fig. 1: Here we plot the data obtained using method (i) in runs with two different concentrations, $c=10$ and $c=0.1$, for different $p$ values ranging from $p=0.0005$ to $p=0.02$. In order to render the comparison easy, we plot in Fig. 1 the normalized velocity $\nu(p)=v(p)/2\sqrt{Dc}$ as a function of $p$; according to classical Fisher kinetics, $\nu(p)$ should behave as $\sqrt{p}$. This classical result for the normalized velocity, $\nu(p)=\sqrt{p}$, is shown in Fig. 1 as a dashed line. We see that the data points for $c=10$ lie slightly above the dashed curve, in line with the theoretical considerations of Refs. [18,19]. On the other hand, the data points for the smaller concentration, $c=0.1$, lie definitely below the dashed curve and tend to it only for extremely small values of $p$. If we try

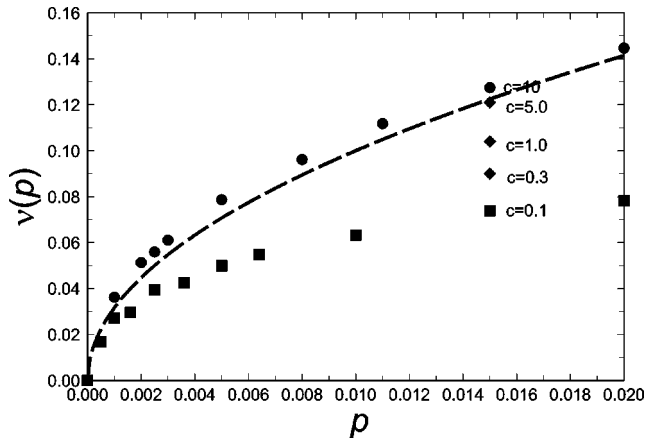


FIG. 1. Normalized front velocity $\nu(p)$ vs the reaction probability $p$ . The dashed curve is the classical solution $\nu(p)=\sqrt{p}$. Numerical results for $c=10$ are given by circles, and for $c=0.1$ by squares. For $p=0.015$ the diamonds give $\nu$ for $c=0.3,1$, and 5.

to describe the data through a power law, i.e., set $\nu(p)\propto p^{\alpha}$, we obtain from a linear fit to $\log_{10}(\nu(p))$ vs $p$ that $\alpha\approx 0.4$. To further elucidate the role of concentration and the nonmonotonic behavior of the actually attained velocity, we plot in Fig. 1 the values of $\nu$ for $p=0.015$ as a function of $c$. We see that at $c=0.1,0.3,1$, and 5 the velocity grows with $c$ but that it stays below the dashed curve, which gives the classical $v_{\min}$. On the other hand, for $c=10$ the velocity exceeds $v_{\min}$ slightly.

For small concentrations, there is no reason for the classical Fisher equation to describe the front velocity correctly: For realizations with relatively large $p$ and in dilute situations (very small $c$), the number of particles within the reaction front is very small, so that the region in which Eq. (9) should start to be applicable contains no $A$ particles. The region is thus certainly not rendered correctly by Eq. (3) and the requirement that the asymptotic solution of Eq.(3) be real (as discussed in Sec. II) is void. On the other hand, when $p$ decreases, the overall number of particles $N=cW=\sqrt{c/2p}$ in the front region increases, so that eventually, at very low $p$, the classical continuous description may become reasonable. Thus, for a given fixed $c$, decreasing $p$ makes the front broader and the number of particles in the front region larger, facts that let $v(p)$ approach $v_{\min}$. Now for large $c$ one finds that $v(p)$ approaches $v_{\min}$ from above [19]. In this work we find that when $c$ is low, the propagation velocity $v(p)$ can be considerably less than $v_{\min}$; it only tends to $v_{\min}$ when $p$ tends to zero, but, interestingly, in this case $v_{\min}$ is not approached from above, but from below.

## IV. THE INTERNAL FRONT STRUCTURE IN THE COMOVING FRAME

Theoretical considerations based on the classical picture rely on the notion of a coordinate frame moving with the front (comoving frame). Operationally, this notion depends on how the front's velocity is defined. In what follows, we compare the results following from definitions (ii) and (iii) since definition (i) is already strongly averaged and does not depict the situation in individual realizations properly [7–9].

As we proceed to show, paralleling [7–9], the ensuing

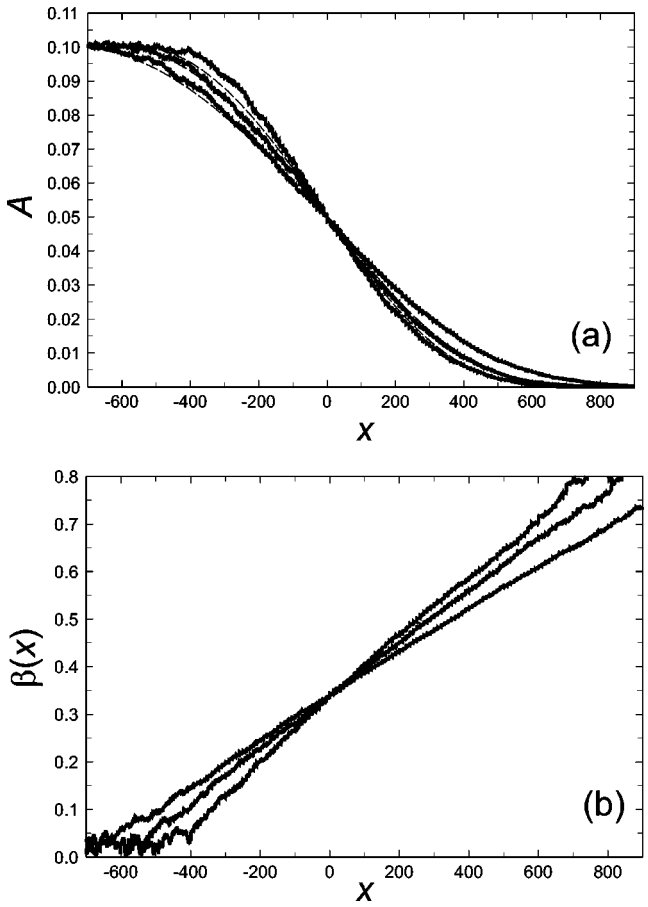


FIG. 2. (a) Concentration profiles in the averaged comoving frame (iii) for $p=0.0025$, 0.005, and 0.01 (left above from left to right). The dashed lines give fits according to Eq. (12), see text for details. (b) $\beta(x)=\sqrt{\log_{10}|\log_{10}(A(x))|}$ vs $x$. The linear behavior in this plot shows in how far Eq. (12) holds.

front forms differ strongly from those obtained by Eq. (3), both near the midpoint of the front and at the front's tail. In Fig. 2(a), we show based on definition (iii) for $p=0.0025$, 0.005, 0.01 (from left to right) the concentration profiles averaged by centering each realization in its comoving frame according to (iii). The front width obtained in this way turns out to be an order of magnitude larger than the Fisher width $W$. In its middle part (near the inflection point) the front is well-represented by a straight line (much better than a Fisher front has to), and then it decays very fast towards it outer tail (leading edge). This decay is not exponential [as it would follow from Eqs. (9) and (11)], but is considerably faster. In fact, a plot of $\log_{10}|\log_{10}(A(x))|$ shows that $A(x)$ decays faster than $e^{-x^n}$ with any $n$, so that both an exponential dependence (as proposed by the Fisher equation) and a Gaussian dependence (as emerging from the simple fluctuation picture) are practically excluded. In Fig. 2(b) we plot $\beta(x)=\sqrt{\log_{10}|\log_{10}(A(x))|}$ vs $x$, and remark that for $x$ large the results are very well rendered by a straight line. This means that for large $x$ the concentration $A(x)$ is

$$A(x)=a\exp\left[-b\exp\frac{(x-x_0)^2}{2\sigma^2}\right]. \qquad (12)$$

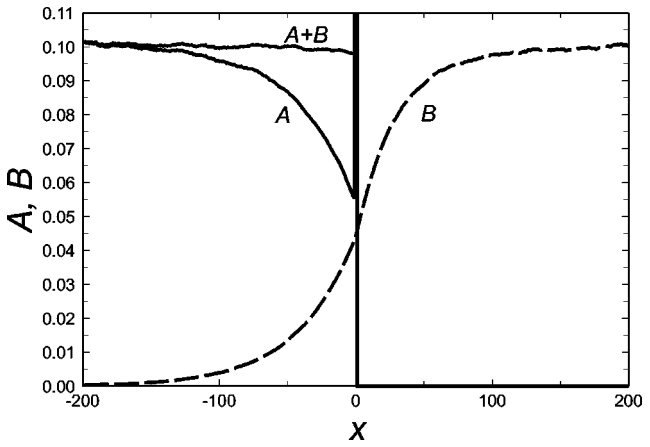


FIG. 3. Front structure in frames centered on the RAP. The dashed line stands for $B(x)$, the full lines for $A(x)$, and for the sum $A(x)+B(x)$. Now $A(x)$ has a $\delta$ peak and $\partial B/\partial x$ a discontinuity at $x=0$. The $A(x)+B(x)$ function is close to constant for $x<0$ and follows $B(x)$ for $x>0$. Note the depletion zone for $B(x)$ for $x>0$.

Note that from our numerical results it follows that Eq. (12) describes very well the behavior of $A(x)$ as long as $x$ is not too small: In Fig. 2(a) we plotted, based on Eq. (12), fits to the numerical data as dashed lines; we obtained these by linear regression in the linear regions of Fig. 2(b). The effective time dependence of the front's width (if any) is extremely weak.

Another way to handle the comoving frame is to center it on the RAP, method (ii). In this case the corresponding density profiles represent the $AB$ and $AA$ correlation functions. This choice gives different information about the front. The behavior which we find in our simulations differs from the one which could be anticipated based on classical kinetics alone, and can only be understood within a discrete particle picture.

Let us study the situation which one sees sitting on the RAP. In Fig. 3 we plot the $A$ and $B$ concentrations averaged in the frames centered on each RAP. Let us first discuss the $A$ concentration. No $A$ particle is to be found to the right from the origin of the coordinates, hence $A(x)=0$ for $x>0$. At $x=0$ the $A(x)$ function shows a $\delta$ peak, due to the RAP. Then for growing, negative $x$ the $A(x)$ shape grows from its dip at $x=0$ to the value $A(x)=C$ to the far left. The $B$ concentration left of the RAP behaves complementarily to $A(x)$, so that $A(x)+B(x)=C=\text{const}$ for $x<0$. For $x>0$, $B(x)$ shows a depletion zone in the vicinity of $x=0$ and tends to $C$ for $x\to\infty$. At $x=0$, $B(x)$ is singular, in that its derivatives left and right of the origin are different.

This singularity is connected with the depletion zone. In the coordinate frame moving with the RAP, the effective diffusion coefficient of all the particles (apart from the RAP) is $\tilde{D}=2D$ (relative diffusion coefficient). The currents of the $B$ particles to the left and right of the RAP differ, due to the probability to react with the RAP, so that

$$\tilde{D}\left(\frac{\partial B_+}{\partial x}-\frac{\partial B_-}{\partial x}\right)=p. \tag{13}$$

We found that at small concentrations and within the numerical accuracy of our simulations, Eq. (13) is correct. For higher concentrations one has to take into account that there can be more than one RAP. The analysis shows that for $c$ large and for small reaction rates, the behavior of $B(x)$ for $x<0$ is rather well reproduced by the intermediate-range solution of the Fisher equation, Eq. (7), but that at larger reaction rates considerable deviations occur.

Thus, both in the (ii) and in the (iii) picture the properties established from simulations differ considerably from the results obtained solely based on Fisher's equation.

## V. CONCLUSIONS

We have considered an autocatalytic reaction scheme with a finite reaction probability in one dimension. We have shown that for very small particle concentrations, the velocities at which the reaction's fronts move are considerably smaller than the minimal propagation velocity obtained in the classical picture, Fisher's Eq. (3). We recover this classical result only for extremely small reaction probabilities. The form of the fronts is related to the type of comoving frame used and the front forms turn out to be very different from the results obtained from Eq. (3).

## ACKNOWLEDGMENTS

We acknowledge support from the DFG, from the GIF I-423 project, and from the Fonds der Chemischen Industrie.

[1] V.N. Kuzovkov and E.A. Kotomin, Rep. Prog. Phys. **51**, 1479 (1988).
[2] E. Kotomin and V. Kuzovkov, *Modern Aspects of Diffusion-Controlled Reactions: Cooperative Phenomena in Bimolecular Processes, in Comprehensive Chemical Kinetics* (Elsevier, Amsterdam, 1996), Vol. 34.
[3] H. Schnörer, V. Kuzovkov, and A. Blumen, Phys. Rev. Lett. **63**, 805 (1989).
[4] G. Zumofen, J. Klafter, and A. Blumen, Phys. Rev. A **44**, 8390 (1991).
[5] J. D. Murray, *Mathematical Biology* (Springer, Berlin, 1979).
[6] P. Gray and S.K. Scott, *Chemical Oscillations and Instabilities* (Clarendon Press, Oxford, 1990).
[7] J. Mai, I.M. Sokolov, and A. Blumen, Phys. Rev. Lett. **77**, 4462 (1996).
[8] J. Mai, V. Kuzovkov, I.M. Sokolov, and A. Blumen, Phys. Rev. E **56**, 4130 (1996).
[9] J. Mai, I.M. Sokolov, and A. Blumen, Europhys. Lett. **44**, 7 (1998).
[10] D.A. Kessler and H. Levine, Nature (London) **394**, 556 (1998).
[11] C.R. Doering, M.A. Bruschka, and W. Horsthemke, J. Stat. Phys. **65**, 953 (1991).
[12] J. Riordan, C.R. Doering, and D. ben-Avraham, Phys. Rev. Lett. **75**, 565 (1995).
[13] H.-P. Breuer, W. Huber, and F. Petruccione, Physica D **73**, 259 (1994).

[14] H.-P. Breuer, W. Huber, and F. Petruccione, Europhys. Lett. **30**, 69 (1995).
[15] M.A. Karzazi, A. Lemarchand, and M. Mareschal, Phys. Rev. E **54**, 4888 (1996).
[16] A. Lemarchand and B. Nowakowski, Europhys. Lett. **41**, 455 (1998).
[17] A. Lemarchand, H. Lemarchand, E. Sulpice, and M. Marechal, Physica A **188**, 277 (1992).
[18] E. Brunet and B. Derrida, Phys. Rev. E **56**, 2597 (1997).
[19] D.A. Kessler, Z. Ner, and L.M. Sander, Phys. Rev. E **58**, 107 (1998).